Geophysical Research Letters

RESEARCH LETTER
10.1029/2024GL108385

The Potential of Absorbing Aerosols to Enhance Extreme Precipitation

Guy Dagan[1] and **Eshkol Eytan**[2,3]

[1]Fredy and Nadine Herrmann Institute of Earth Sciences, Hebrew University, Jerusalem, Israel, [2]Chemical Sciences Laboratory, National Oceanic and Atmospheric Administration, Boulder, CO, USA, [3]Cooperative Institute for Research in Environmental Sciences, University of Colorado Boulder, Boulder, CO, USA

Key Points:

- The effect of absorbing aerosol on extreme precipitation is examined in idealized convective-resolving radiative-convective-equilibrium simulations
- Aerosol perturbation that shifts the lower tropospheric radiative heating rate to positive values strongly enhances extreme precipitation
- This trend is explained by a mechanism reported before for hothouse climate conditions involving a shift into an "episodic deluge" regime

Supporting Information:

Supporting Information may be found in the online version of this article.

Correspondence to:

G. Dagan,
guy.dagan@mail.huji.ac.il

Citation:

Dagan, G., & Eytan, E. (2024). The potential of absorbing aerosols to enhance extreme precipitation. *Geophysical Research Letters*, *51*, e2024GL108385. https://doi.org/10.1029/2024GL108385

Received 25 JAN 2024
Accepted 6 APR 2024

Author Contributions:

Conceptualization: Guy Dagan
Formal analysis: Guy Dagan, Eshkol Eytan
Methodology: Guy Dagan, Eshkol Eytan
Visualization: Guy Dagan
Writing – original draft: Guy Dagan
Writing – review & editing: Guy Dagan, Eshkol Eytan

Abstract Understanding the impact of various climate forcing agents, such as aerosols, on extreme precipitation is socially and scientifically vital. While anthropogenic absorbing aerosols influence Earth's energy balance and atmospheric convection, their role in extreme events remains unclear. This paper uses convective-resolving radiative-convective-equilibrium simulations, with fixed solar radiation, to investigate the influence of absorbing aerosols on extreme precipitation comprehensively. Our findings reveal an underappreciated mechanism through which absorbing aerosols can, under certain conditions, strongly intensify extreme precipitation. Notably, we demonstrate that a mechanism previously reported for much warmer (hothouse) climates, where intense rainfall alternates with multi-day dry spells, can operate under current realistic conditions due to absorbing aerosol influence. This mechanism operates when an aerosol perturbation shifts the lower tropospheric radiative heating rate to positive values, generating a strong inhibition layer. Our work highlights an additional potential effect of absorbing aerosols, with implications for climate change mitigation and disaster risk management.

Plain Language Summary Aerosols, particles suspended in the atmosphere, can interact with the incoming solar radiation by scattering or absorbing it. Aerosol species that absorb solar radiation generate local warming of the atmosphere. This local warming changes the vertical profile of temperature and by that affects cloud and precipitation development. In this paper we use idealized computer simulations to investigate the effect of absorbing aerosols on precipitation, and specifically on extreme precipitation events in the tropics. We demonstrate that under certain conditions, absorbing aerosols can strongly enhance extreme precipitation even despite reducing the mean. We show that this trend can be explained by a mechanism previously reported for much warmer climate conditions than currently found on Earth, involving heating by radiation of the lower part of the troposphere. These results have implications for climate change mitigation and disaster risk management.

1. Introduction

Precipitation is a fundamental component of Earth's climate system, shaping regional hydrology, ecosystem dynamics, and human societies. Understanding the intricate processes that govern precipitation is crucial for addressing water resource management, flood risks, and climate change impacts. Recent research has highlighted the significant role of aerosols, particularly absorbing aerosols, in modulating the energy budget of the atmosphere and subsequently influencing precipitation patterns (Dagan et al., 2019; Herbert et al., 2021; Liu et al., 2018; Samset, 2022; Sand et al., 2020; Williams et al., 2023). Absorbing aerosols, such as black carbon (Bond et al., 2013), possess the ability to absorb solar radiation and alter the vertical temperature gradient (Lu et al., 2020; Stjern et al., 2017; Wilcox et al., 2016), thereby perturbing the convective dynamics and thermodynamic conditions conducive to precipitation.

Extreme precipitation events, characterized by strong intensity and potential for severe flooding, have garnered increased attention due to their societal and environmental implications (i.e., (Abbott et al., 2020; Ban et al., 2015; Emori & Brown, 2005; Pendergrass et al., 2015; Sillmann et al., 2019; Tabari, 2020)). Understanding the underlying mechanisms of extreme precipitation events is essential for adapting to a changing climate where such events may become more frequent or intense (Allan et al., 2020; Goswami et al., 2006). Recent studies (Fan et al., 2015; Z. Li et al., 2019; Sillmann et al., 2019; T. Wang et al., 2015) have suggested that absorbing aerosols can play a non-negligible role in modulating extreme precipitation events. However, the precise mechanisms through which absorbing aerosols influence extreme precipitation, and the extent to which they do so, remain

uncertain. For example, in global climate models, the inter-model spread of the responses of extreme precipitation to black-carbon was demonstrated to be large compared with other external forcings (Sillmann et al., 2019).

Unlike extreme precipitation, the response of global mean precipitation to an absorbing aerosol perturbation is better understood by the atmospheric energy budget perspective (Allan et al., 2020; Dagan et al., 2019; Liu et al., 2018; O'Gorman et al., 2012; Sand et al., 2020). According to this perspective, the mean precipitation, which act to warm the atmosphere by latent heat release, is determined by the ability of the atmosphere to radiatively cool (with a small contribution from surface sensible heat flux). Thus, an absorbing aerosol perturbation, which radiatively warm the atmosphere, act to reduce the mean precipitation (Dagan et al., 2019; McCoy et al., 2022; Ming et al., 2010; Myhre et al., 2018; Persad, 2023; Samset, 2022; Sand et al., 2020; Sillmann et al., 2019; Zhang et al., 2021). It was shown that the energetic argument holds for large temporal and spatial scales (Dagan & Stier, 2020; Jakob et al., 2019). However, it should be noted that this argument does not provide specific insights into the temporal distribution of precipitation, thus it is not informative regarding extreme precipitation responses.

In a seemingly unrelated context to absorbing aerosols, recent research has demonstrated that under hothouse climate conditions—warmer than our current climate, believed to have existed in the distant history of our planet—precipitation shifts from the quasi-equilibrium condition observed today to an "episodic deluge" regime. This regime is characterized by short and intense outbursts of rainfall separated by multi-day dry spells (Dagan et al., 2023; Seeley & Wordsworth, 2021; Song et al., 2023; Spaulding-Astudillo & Mitchell, 2023).

The transition into the "episodic deluge" regime has been attributed to the radiative effect of water vapor (Seeley & Wordsworth, 2021). Specifically, under these warmer conditions (exceeding current average surface temperatures by a few tens of degrees), the water vapor concentration in the lower troposphere increases, such that the water vapor infrared window becomes opaque (Wolf & Toon, 2015; kumar Kopparapu et al., 2016; Popp et al., 2016; Wolf et al., 2018; Seeley & Wordsworth, 2021). This closure of the infrared window shifts the lower-tropospheric radiative cooling, observed in the current climate, into weak radiative warming (Seeley & Wordsworth, 2021; Wolf et al., 2018). Consequently, lower-tropospheric radiative heating (LTRH) induces convective inhibition (Seeley & Wordsworth, 2021; Wolf et al., 2018), initially suppressing convection. Simultaneously, upper troposphere radiative cooling and surface fluxes work to increase convective instability in the absence of convection, leading to its gradual accumulation. The instability, measured by temperature lapse-rate or near-surface moist-static energy (MSE), builds up until latent cooling of the inhibition layer by virga enables the development of a strong and short-lived convection event that consumes the instability (Seeley & Wordsworth, 2021), followed by an additional dry period.

Using radiative-convective-equilibrium (RCE) simulations with idealized and prescribed radiative heating rate vertical profiles, it was shown that LTRH under current tropical sea surface temperature (SST) could also generate a shift into episodic deluge regime (Dagan et al., 2023; Seeley & Wordsworth, 2021; Song et al., 2023). Hence, it was speculated that LTRH due to an absorbing aerosol perturbation in the tropics could affect extreme precipitation under our current climate conditions (Dagan et al., 2023). This paper aims to examine this speculation and provide a comprehensive examination of the impact of absorbing aerosols on tropical precipitation in RCE simulations (which exclude diurnal cycle), with a particular focus on extreme precipitation events.

2. Methods

2.1. Model Description and Experimental Design

The System for Atmospheric Modeling (SAM) version 6.11.8 is used in this study (Khairoutdinov & Randall, 2003). Smagorinsky's eddy diffusivity model is employed to parameterize subgrid-scale fluxes, and a 2-moment bulk scheme represents cloud microphysics (Morrison et al., 2005). The activation of cloud condensation nuclei (CCN) at the cloud base is parameterized using the vertical velocity and CCN spectrum parameters (Twomey, 1959). The CCN concentration activated at 1% supersaturation is prescribed to be 200 cm^{-3} in all simulations, that is, we are focusing here only on aerosol-radiation interactions and not aerosol-cloud interactions. In the baseline simulations, which run with interactive radiation, longwave and shortwave radiative fluxes are calculated using the RRTMG radiation scheme every 5 min (Clough et al., 2005; Iacono et al., 2008; Mlawer et al., 1997).

Our simulations adhere to the RCEMIP (RCE Model Inter-comparison Project) small-domain protocol (Wing et al., 2018). Conducted on a square, doubly periodic domain measuring 96×96 km^2, this size is chosen to prevent convective self-aggregation (Muller & Held, 2012). The horizontal and vertical grids follow the RCEMIP protocol, with a 1 km horizontal grid spacing and 74 vertical levels spanning from 37m to 33 km. A 10s time step is utilized, and each simulation runs for 150 days, with the final 50 days dedicated to analysis. Trace gas concentrations and initial conditions mirror those presented in Wing et al. (2018). Similarly, following Wing et al. (2018), a fixed-in-time solar insulation is used, that is, no diurnal cycle is considered. Three distinct prescribed SSTs are considered: 295, 300, and 305K. Domain mean clouds, precipitation and radiation properties of these baseline simulations (i.e., excluding aerosol absorption) are presented in Figure S1 in Supporting Information S1. In addition, the reader is referred to Lorian and Dagan (2023) for further details about clouds, precipitation and radiation properties in similar simulations.

2.2. Aerosol Radiative Effect Calculations

To represent the radiative impact of aerosols, we utilize the Max Planck Institute Aerosol Climatology version 2, Simple Plume (MACv2-SP) parametrization, incorporating vertical distributions and optical property parameters of biomass-absorbing aerosols (Stevens et al., 2017). Derived from observations (Kinne et al., 2013), MACv2-SP efficiently characterizes spatiotemporal distributions of anthropogenic aerosol optical properties. This parametrization includes four biomass aerosol plumes situated over North Africa, South America, the Maritime Continent (around Indonesia), and Central Africa, each featuring a distinct vertical distribution capturing a spectrum of realistic conditions (Figure 1a). Previous studies have highlighted the influence of the vertical location of absorbing aerosols on atmospheric responses (Ming et al., 2010; Ban-Weiss et al., 2012; Persad et al., 2012; Kim et al., 2015; Z. Wang et al., 2018; Slater et al., 2022). Thus, we employ four realistic vertical profiles to assess the sensitivity of extreme precipitation responses. To explore the sensitivity of precipitation to aerosol perturbation, we vary the total aerosol optical depth (AOD) at 0.55 μm across four levels: 0.1, 0.25, 0.5, and 0.75, encompassing a broad yet realistic range of conditions (Holben et al., 2001; Kinne et al., 2013).

The MACv2-SP absorbing aerosol profiles (Figure 1a) serve as the foundation for offline radiative transfer model calculations using the Santa Barbara DISORT Atmospheric Radiative Transfer (SBDART) model (Ricchiazzi et al., 1998). The radiative heating rate (RHR) attributed to the introduction of absorbing aerosols is determined by the difference between simulations conducted with and without absorbing aerosols using SBDART (Figure 1b).

Specifically, the aerosol RHR is modeled using SBDART's user-defined spectral dependence mode. The aerosol single scattering albedo, extinction efficiency, and asymmetry factor are defined at four wavelengths (0.44, 0.67, 0.87, 1.0 μm) and interpolate and extrapolate to the rest of the spectrum (logarithmically for the extinction according to Angstrom exponent model and linearly for all others). The model is run for wavelengths ranging from 0.25 to 100 μm in resolution of 0.005 μm. The spectral information is used as heating rates are derived from the entire spectrum; here we take a data-driven approach for the representation of the spectral properties, rather than the analytical equations used by Stevens et al. (2017). The biomass burning aerosol spectral information is taken from AERONET retrievals (Dubovik et al., 2000) of a biomass burning event that was measured on the Reunion island (near Madagascar) on the 25th of September 2017, and shows good agreement with the properties reported by Stevens et al. (2017) for the 0.55 μm wavelength and the monochromatic properties reported by Shi et al. (2019). The scattering phase function is modeled using the Henyey-Greenstein approximation, which was shown to hold very well (and mostly) for biomass-burning particles (J. Li et al., 2015). The 1D radiation transfer model is run for a typical tropical atmospheric profile with a solar zenith angle of 55° and a Lambertian spectrally dependent surface albedo model of seawater built-in SBDART. Sensitivity tests demonstrate that the effect of aerosol on the RHR vertical profile only weakly depends on the baseline thermodynamic conditions in the range examined here. Thus, we use the same radiative calculations to represent the aerosol effect in the different SST scenarios. We note that the estimated RHR presented in Figure 1b aligns qualitatively in magnitude and vertical structure with observed RHR profiles from previous studies on absorbing aerosols (Z. Wang et al., 2018; Lu et al., 2020; Fasano et al., 2021; Cochrane et al., 2022).

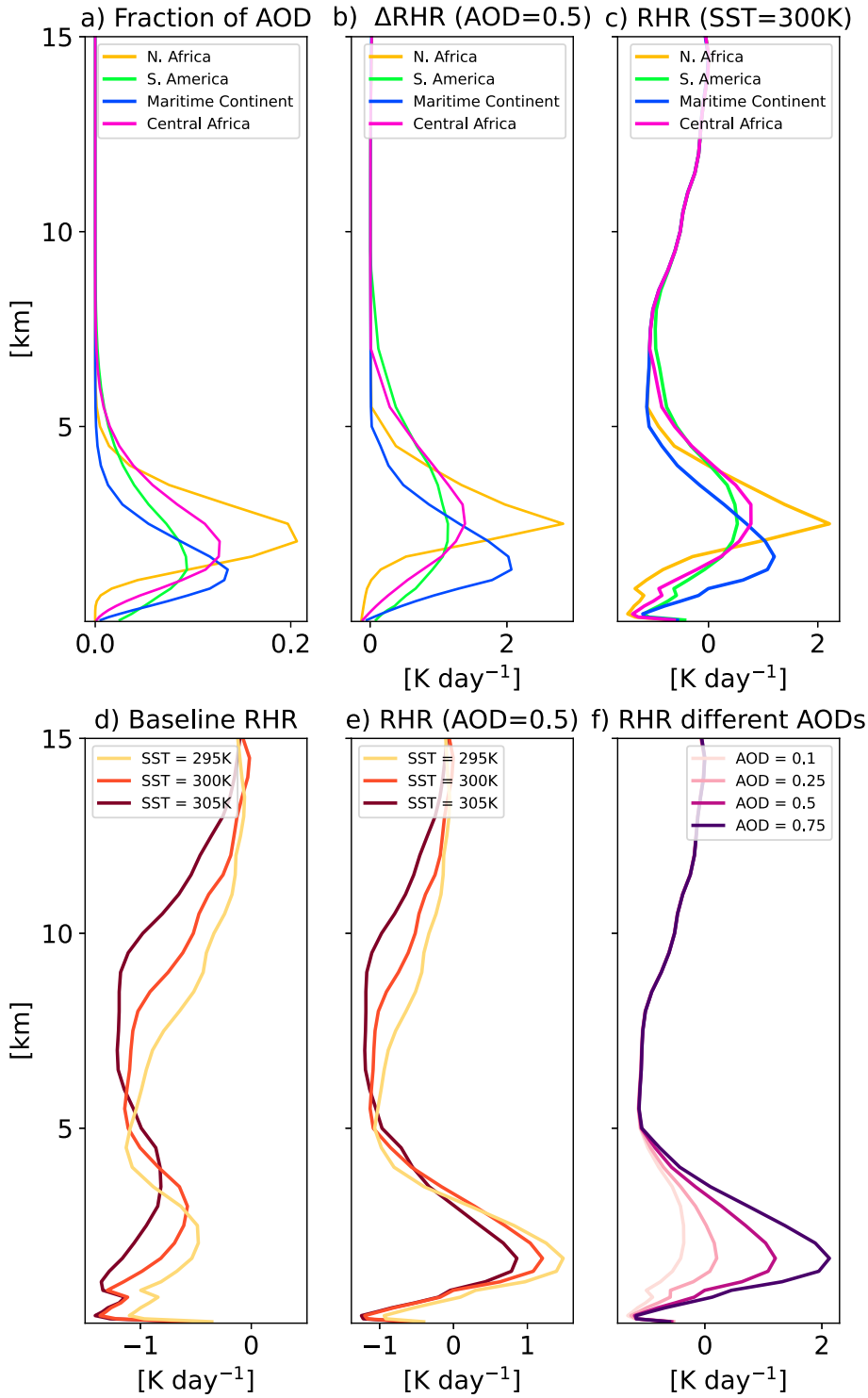

Figure 1. Vertical profiles of: (a) fractional aerosol optical depth (AOD) in various absorbing aerosol plumes, (b) radiative effects of different aerosol plumes assuming AOD = 0.5, (c) total radiative heating rate (RHR) in simulations with SST = 300K and AOD = 0.5 for different aerosol vertical profiles, (d) RHR in baseline simulations excluding aerosol radiative effects under various SSTs, (e) RHR in simulations with different SSTs and AOD = 0.5, assuming the Maritime Continent vertical profile, and (f) RHR in simulations with SST = 300K, assuming the Maritime Continent vertical profile, but with different AODs.

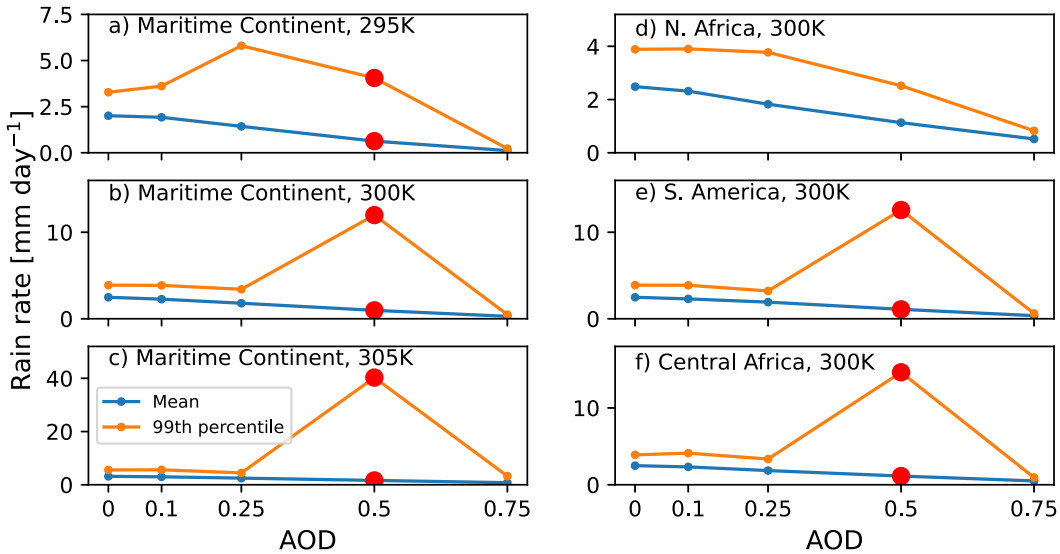

Figure 2. Domain- and time-mean, and 99th percentile rain rates as functions of AOD for various simulations. Panels (a–c) depict simulations using the Maritime Continent aerosol vertical profile under different SSTs, while panels (d–f) show simulations using different aerosol vertical profiles under SST = 300K. Red markers indicate simulations characterized by precipitation occurring in episodic deluges ($\eta \geq 1$).

2.3. Integrating SBDART RHR Into RCE Simulations

The vertical profiles of absorbing aerosol radiative heating rates (ΔRHR; Figure 1b) are incorporated into baseline RHR profiles obtained from RCE simulations with different SSTs and interactive radiation calculations, excluding aerosol effects (Figure 1d). These modified RHR profiles, now accounting for the aerosol radiative effect, serve as inputs for RCE simulations with prescribed radiation. Each aerosol plume, originating from a different geographic location and featuring a distinct vertical structure (Figure 1b), is employed in separate RCE simulations assuming SST = 300K (Figure 1c illustrates the RHR used in simulations with different aerosol vertical profiles and AOD = 0.5, as an example). Furthermore, to assess the sensitivity of the results to baseline SST conditions, simulations are conducted with a single aerosol vertical profile (the Maritime Continent plume) under three different SSTs (see Figure 1e, for example).

For each aerosol plume and SST condition considered, four simulations are executed with the four AOD levels mentioned above (see Figure 1f, for example). In total, 27 simulations are conducted, comprising three baseline simulations under different SSTs, 16 simulations for four different aerosol vertical profiles under four different AODs and SST = 300K, and eight additional simulations for two additional SSTs with one aerosol vertical profile (Maritime Continent plume), each using four different AODs.

3. Results and Discussion

We begin our analysis by investigating both the time-mean and extreme precipitation across various simulations (Figure 2). As anticipated from the energetic perspective (Allan et al., 2020; Dagan et al., 2019; O'Gorman et al., 2012), there is a consistent reduction in domain- and time-mean precipitation with an increase in absorbing aerosol AOD. Surprisingly, despite the decline in mean precipitation, Figure 2 reveals a non-monotonic trend in extreme precipitation (defined here as the 99th percentile domain-mean hourly precipitation; the general results do not differ for different thresholds within a reasonable range). Specifically, under medium-high AOD levels (0.5), extreme precipitation is notably enhanced in the majority of cases examined here, distinguishing it from other AOD levels.

The occurrence of substantial extreme precipitation without a concurrent increase in the mean precipitation suggests heightened variability over time. This variability can be quantified using the relative dispersion, denoted as η, defined as the ratio of the standard deviation to the mean. A recent study has associated a quasi-steady

precipitation regime with $\eta \ll 1$, while an "episodic deluge" regime is characterized by $\eta \geq 1$ (Dagan et al., 2023). In Figure 2, simulations displaying $\eta \geq 1$ are highlighted with a red marker.

Under an AOD of 0.5, where the lower tropospheric RHR shifts to positive values (Figure 1f), all three examined SSTs under the Maritime Continent vertical profile exhibit $\eta \geq 1$ (Figures 2a–2c), as well as in three out of the four vertical profiles considered (Figures 2b and 2d–2f). In conditions of the highest AOD (0.75), precipitation is largely suppressed, leading to a corresponding reduction in extreme precipitation. This behavior aligns with the energetic perspective, where under high AOD conditions, the vertically integrated RHR approaches positive values (Figure 1f), preventing precipitation and its associated latent heating.

For relatively low AODs ($\leq$0.25), the aerosol perturbation is insufficient to shift the lower tropospheric RHR significantly to positive values (Figure 1f), thus preventing the transition to an episodic deluge regime (i.e., $\eta \ll 1$). An exception occurs under an SST of 295K and an AOD of 0.25, where η is close to, but smaller than, 1 (=0.9). In this simulation, an increase in extreme precipitation is observed compared to lower AOD conditions (Figure 2a). This occurs as the RHR in the baseline conditions at the lower troposphere is weaker (i.e., less negative) under SST of 295K compared with higher SSTs (Figure 1d). Thus, an AOD of 0.25 is sufficient to transform the lower tropospheric RHR to positive values (Figure S2 in Supporting Information S1), which in turn, derive the increase in extreme precipitation. These results suggest that the baseline RHR conditions play a role in the response to absorbing aerosol perturbation.

To gain a deeper understanding of the extreme precipitation response to absorbing aerosols, we delve into the time series and distribution function of precipitation in simulations conducted with AOD = 0.5 and without aerosol radiative effect (AOD = 0). This is done for the different aerosol vertical profiles and different SSTs examined here, as depicted in Figure 3. The figure illuminates how the introduction of absorbing aerosols transforms rainfall dynamics from a quasi-steady regime observed under clean conditions, characterized by a relatively narrow distribution, to an episodic deluge regime, characterized by a much wider distribution with a maximum near zero and a long positive tail. The episodic deluge regime is characterized by regular, brief, and intense bursts of rainfall, separated by rain-free intervals across the entire domain. This regime transition holds for all cases examined, except for the North African vertical profile (Figure 3d), which demonstrates a general reduction in the mean precipitation with a shift in the distribution to smaller rain rates under a fixed distribution shape. The North African aerosol plume, positioned higher in the atmosphere compared to others (Figure 1a), induces warming concentrated around 3 km height, with minimal impact near the surface (Figures 1b and 1c). Consequently, this plume does not generate the pronounced inhibition and decoupling observed in other plumes (further details are provided below; see also Figure 2d).

Figure 3 also highlights that, under the Maritime Continent vertical profile, an increase in SST correlates with a reduction in the frequency of rain events and an increase in their characteristic magnitude. A recent study has shown that the period of the episodic deluges can be predicted by considering the time for radiation and re-evaporation to cool the lower atmosphere (Song et al., 2023), a factor expected to vary with SST. Furthermore, it has been demonstrated that, even under the same RHR vertical profile, higher SST facilitates a smoother transition into the episodic deluge regime (Dagan et al., 2023). Additionally, it is worth noting that to maintain the domain-mean energy constraint, a decrease in the frequency of rain events should be accompanied by an increase in their magnitudes.

Figure 4 illustrates the underlying physical processes contributing to the episodic deluge regime in simulations incorporating aerosol absorption. It highlights that the mechanism identified by Seeley and Wordsworth (2021) for hothouse climate conditions also operates under the influence of absorbing aerosols in the current climate. Specifically, as depicted in Figure 4, this oscillatory pattern consists of three main phases, as explained by Seeley and Wordsworth (2021): the recharge phase, the triggering phase, and the discharge phase.

During the discharge phase, characterized by episodes of heavy precipitation (i.e., exceeding 5 mm hr^{-1}), the lower troposphere becomes filled with air having low MSE (see Figure 4e). As the instability is depleted, the recharge phase begins (defined here to commence when the rain rate falls below 5 mm hr^{-1}). In the recharge phase the surface is decoupled from the upper troposphere by an inhibition layer (Fan et al., 2015; Slater et al., 2022; Wilcox et al., 2016), which becomes warmer and more stable with time (Figure 4c) due to radiative heating of this layer (Figure 1c). This decoupling inhibits surface convection, preventing the ventilation of near-surface air (Ding et al., 2016; Slater et al., 2022; Stjern et al., 2023; Wilcox et al., 2016), which accumulates MSE from surface

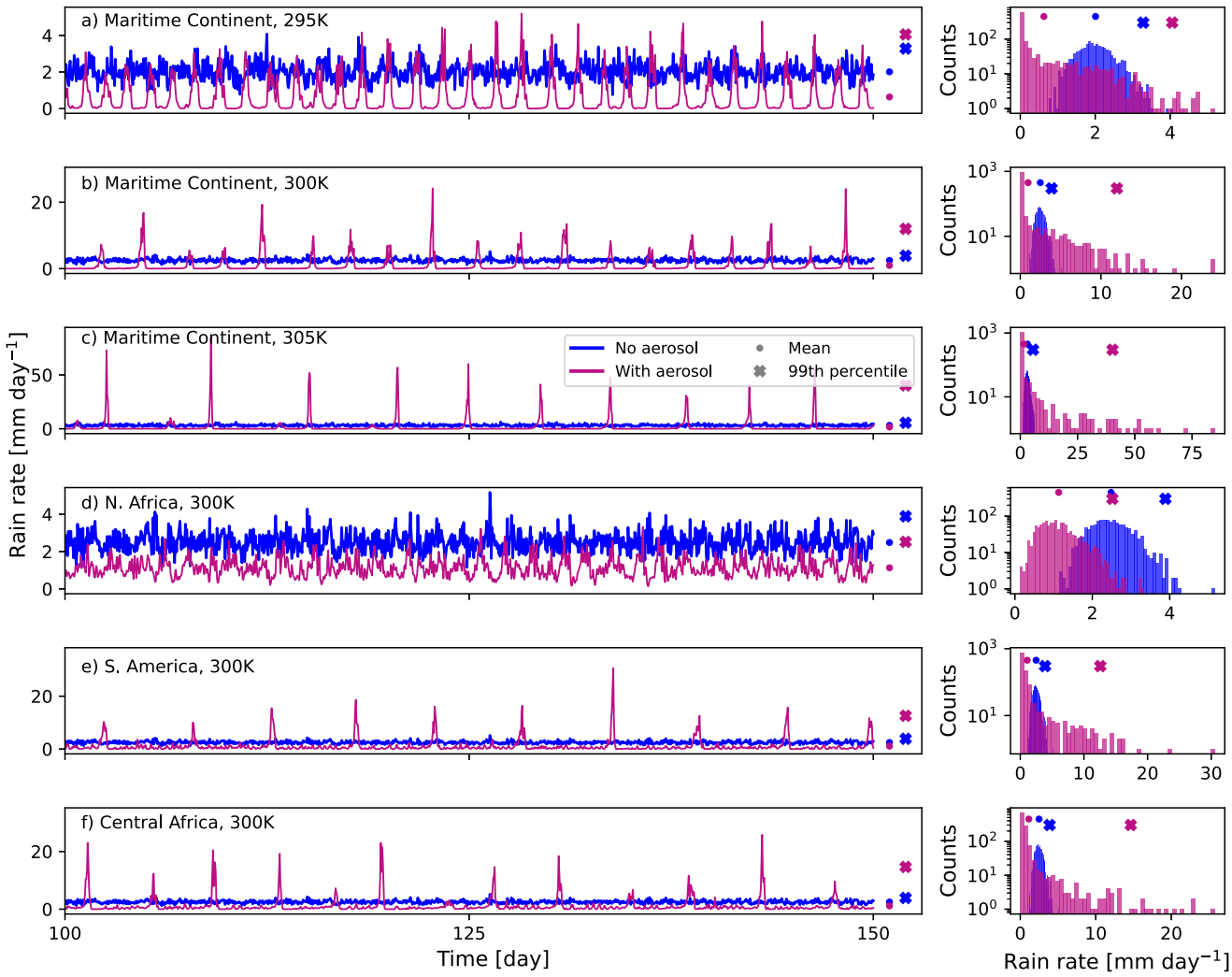

Figure 3. Time series of the domain-mean rain rate in different simulations conducted without or with aerosol radiative effect (the different colors). (a–c) Results of simulations conducted under different sea surface temperatures and with the Maritime Continent vertical profile. (d–f) Results of simulations conducted under different vertical profiles of absorbing aerosol. The simulations which include the aerosol radiative effect presented here are conducted with an aerosol optical depth of 0.5. The time mean and extreme (99th percentile) rain rate are presented on the right side of each panel as dots and Xs, respectively. The time mean precipitation of these simulations also appears in Table S1 in Supporting Information S1, for clarity. The full histogram of rain rates is presented on the right. Note the different *y*-axis range in the different panels.

fluxes (see Figure 4e). Simultaneously, radiation acts to cool the upper troposphere (see Figure 1c), and in conjunction with surface fluxes, results in a substantial buildup of convective instability. Over the course of a few days, this buildup makes the atmosphere highly susceptible to intense precipitation events.

During the triggering phase (defined as the stage in which $\frac{d\theta_{inhibt.}}{dt} < 0$ K hr^{-1} and the rain rate is < 5 mm hr^{-1}), the inhibition becomes weaker with time due to evaporation cooling (Seeley & Wordsworth, 2021, Figure 4c). This cooling is caused by the precipitating water that appears at the mid-troposphere at the beginning of the triggering phase (Figure 4b) leading to virga, as was shown in Seeley and Wordsworth (2021). This serves as a trigger, allowing surface-based convection to reach the upper troposphere (Figures 4a and 4b), which drives the initiation of the discharge phase again, lasting for a few hours until enough instability is consumed.

4. Conclusions

Through km-scale RCE simulations, we explore the impact of absorbing aerosols on tropical precipitation, with a specific focus on extreme events. Our findings reveal that, under certain conditions, absorbing aerosols can

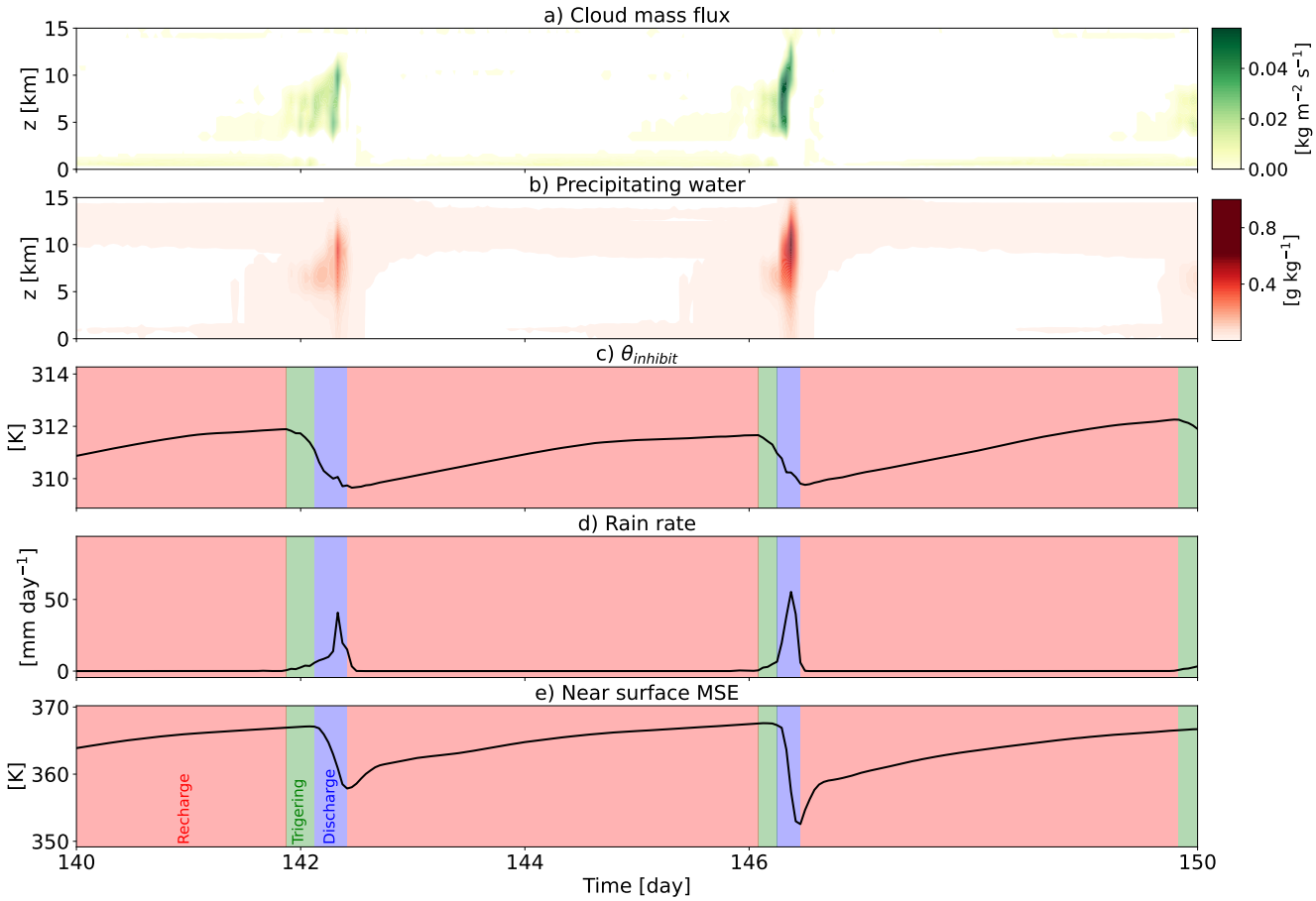

Figure 4. Time series of domain-mean (a) cloud upward mass flux, (b) precipitation water content, (c) potential temperature of the inhibition layer (θ_{inhibt}) defined at a height of 1500m above the surface, (d) surface rain rate, and (e) near-surface moist-static energy (MSE). The results presented here are from the last 10 days of a radiative-convective equilibrium simulation using the Maritime Continent absorbing aerosol vertical profile with an aerosol optical depth of 0.5 and a sea surface temperature of 305K.

significantly enhance extreme precipitation, even while reducing the mean. This phenomenon can be explained by a mechanism previously reported for much warmer climate conditions than those currently present on Earth, involving radiation-induced heating of the lower troposphere. In these conditions, lower-tropospheric radiative heating (LTRH) induces convective inhibition (Seeley & Wordsworth, 2021; Slater et al., 2022; Wilcox et al., 2016; Wolf et al., 2018), while radiative cooling in the upper troposphere heightens convective instability. The absence of convection, due to strong inhibition and decoupling of the surface layer, allows convective instability to accumulate, rendering the atmosphere highly susceptible to intense precipitation events. Eventually, latent cooling weakens the inhibition layer, triggering robust convection and a precipitation event that consumes the accumulated instability. This cycle repeats, with each precipitation event lasting only a few hours.

The distinction between hothouse climate conditions and the impact of absorbing aerosols lies in the source of lower-tropospheric radiative heating (LTRH). In hothouse climates, LTRH is induced by water vapor, affecting mainly the longwave part of the spectrum. Conversely, in the case of absorbing aerosols, LTRH results from shortwave absorption by the aerosols. Nevertheless, our findings indicate that the outcomes can be similar in terms of precipitation distribution.

Our results further demonstrate that for getting an increase in extreme precipitation with absorbing aerosol perturbation, the perturbation must be substantial enough to shift the lower tropospheric RHR to positive values. However, it should not be so extreme that the vertically integrated RHR reaches positive values, which would lead to the complete suppression of precipitation. Moreover, we show that this phenomenon does not manifest when the aerosols are predominantly located well above the surface, as this warming does not effectively decouple the

surface from the free troposphere. This mechanism, and the characteristics of the rain cycles, also appear to be sensitive to the baseline SST conditions.

It is important to note that our simulations, which include aerosol radiative perturbation are not directly coupled to radiation (i.e., using prescribed radiation based on offline radiative transfer calculations). This may introduce some uncertainties in our findings that should be addressed in future work. In addition, the idealized setup used here does not include diurnal cycle in the shortwave radiations, which could affect our finding to some degree (Herbert et al., 2021). Specifically, we speculate that in a more realistic setup, heat that is accumulated during the day will be counteracted by stronger radiative cooling during the night. However, the idealized nature of this study facilitates a physical understanding of the underlined processes, which will be examined in the future in more comprehensive frameworks. Additionally, the fact that we use small domain simulations, the absence of large-scale circulation effects and the use of a fixed SST in our simulations should be considered as potential limitations in the scope of our results. These factors warrant further investigation and may refine our understanding of the relationship between absorbing aerosols and extreme precipitation (e.g., see Dagan et al. (2023) for large domain simulations of hothouse climate episodic deluges regime). Furthermore, previous studies using global climate simulations (Dagan et al., 2021; Persad, 2023; Williams et al., 2023) demonstrated that the location of the absorbing aerosol perturbation matters for the local- and global-mean precipitation response. Thus, it will also be interesting to examine the response of extreme precipitation to different geographical locations of aerosol perturbation in global convective-resolving simulations.

Our results suggest a novel mechanism by which anthropogenic forcing could affect extreme precipitation events. Extreme precipitation events are of high social and scientific interest due to their destructive potential. Thus, our results could have impotent implications for disaster risk management.

Data Availability Statement

The model SAM is publicly available in Khairoutdinov (2023). The aerosol spectral radiative properties are freely available at: https://aeronet.gsfc.nasa.gov. The data used here is take from the measurements conducted at Reunion island on the 25th of September 2017. The modeled data presented in this study is publicly available in https://zenodo.org/doi/10.5281/zenodo.10457482 (Dagan & Eytan, 2024).

Acknowledgments
This research has been supported by the German Research Foundation (DFG) under Grant HO 6588/3-1. E. Eytan was supported by the CIRES Visiting Fellows Program, funded by NOAA Cooperative Agreement NA22OAR4320151. E. Eytan is thankful for the help of the Institute for Environmental Sustainability (IES) at the Weizmann Institute of Science. The authors thank Marat Khairoutdinov for providing SAM.

References

Abbott, T. H., Cronin, T. W., & Beucler, T. (2020). Convective dynamics and the response of precipitation extremes to warming in radiative–convective equilibrium. *Journal of the Atmospheric Sciences*, *77*(5), 1637–1660. https://doi.org/10.1175/jas-d-19-0197.1

Allan, R. P., Barlow, M., Byrne, M. P., Cherchi, A., Douville, H., Fowler, H. J., et al. (2020). Advances in understanding large-scale responses of the water cycle to climate change. *Annals of the New York Academy of Sciences*, *1472*(1), 49–75. https://doi.org/10.1111/nyas.14337

Ban, N., Schmidli, J., & Schär, C. (2015). Heavy precipitation in a changing climate: Does short-term summer precipitation increase faster? *Geophysical Research Letters*, *42*(4), 1165–1172. https://doi.org/10.1002/2014gl062588

Ban-Weiss, G. A., Cao, L., Bala, G., & Caldeira, K. (2012). Dependence of climate forcing and response on the altitude of black carbon aerosols. *Climate Dynamics*, *38*(5–6), 897–911. https://doi.org/10.1007/s00382-011-1052-y

Bond, T. C., Doherty, S. J., Fahey, D. W., Forster, P. M., Berntsen, T., DeAngelo, B. J., et al. (2013). Bounding the role of black carbon in the climate system: A scientific assessment. *Journal of Geophysical Research: Atmospheres*, *118*(11), 5380–5552. https://doi.org/10.1002/jgrd.50171

Clough, S., Shephard, M., Mlawer, E., Delamere, J., Iacono, M., Cady-Pereira, K., et al. (2005). Atmospheric radiative transfer modeling: A summary of the aer codes. *Journal of Quantitative Spectroscopy and Radiative Transfer*, *91*(2), 233–244. https://doi.org/10.1016/j.jqsrt.2004.05.058

Cochrane, S. P., Schmidt, K. S., Chen, H., Pilewskie, P., Kittelman, S., Redemann, J., et al. (2022). Biomass burning aerosol heating rates from the oracles (observations of aerosols above clouds and their interactions) 2016 and 2017 experiments. *Atmospheric Measurement Techniques*, *15*(1), 61–77. https://doi.org/10.5194/amt-15-61-2022

Dagan, G., & Eytan, E. (2024). Data for the paper: Absorbing aerosols can strongly enhance extreme precipitation [Dataset]. *Zenodo*. https://zenodo.org/doi/10.5281/zenodo.10457482

Dagan, G., Seeley, J. T., & Steiger, N. (2023). Convection and convective-organization in hothouse climates. *Journal of Advances in Modeling Earth Systems*, *15*(11), e2023MS003765. https://doi.org/10.1029/2023ms003765

Dagan, G., & Stier, P. (2020). Constraint on precipitation response to climate change by combination of atmospheric energy and water budgets. *npj Climate and Atmospheric Science*, *3*(1), 1–5. https://doi.org/10.1038/s41612-020-00137-8

Dagan, G., Stier, P., & Watson-Parris, D. (2019). Contrasting response of precipitation to aerosol perturbation in the tropics and extratropics explained by energy budget considerations. *Geophysical Research Letters*, *46*(13), 7828–7837. https://doi.org/10.1029/2019gl083479

Dagan, G., Stier, P., & Watson-Parris, D. (2021). An energetic view on the geographical dependence of the fast aerosol radiative effects on precipitation. *Journal of Geophysical Research: Atmospheres*, *126*(9), e2020JD033045. https://doi.org/10.1029/2020jd033045

Ding, A., Huang, X., Nie, W., Sun, J., Kerminen, V.-M., Petäjä, T., et al. (2016). Enhanced haze pollution by black carbon in megacities in China. *Geophysical Research Letters*, *43*(6), 2873–2879. https://doi.org/10.1002/2016gl067745

Dubovik, O., Smirnov, A., Holben, B., King, M., Kaufman, Y., Eck, T., & Slutsker, I. (2000). Accuracy assessments of aerosol optical properties retrieved from aerosol robotic network (aeronet) sun and sky radiance measurements. *Journal of Geophysical Research*, *105*(D8), 9791–9806. https://doi.org/10.1029/2000jd900040

Emori, S., & Brown, S. (2005). Dynamic and thermodynamic changes in mean and extreme precipitation under changed climate. *Geophysical Research Letters*, *32*(17), L17706. https://doi.org/10.1029/2005gl023272

Fan, J., Rosenfeld, D., Yang, Y., Zhao, C., Leung, L. R., & Li, Z. (2015). Substantial contribution of anthropogenic air pollution to catastrophic floods in southwest China. *Geophysical Research Letters*, *42*(14), 6066–6075. https://doi.org/10.1002/2015gl064479

Fasano, G., Diémoz, H., Fountoulakis, I., Cassardo, C., Kudo, R., Siani, A. M., & Ferrero, L. (2021). Vertical profile of the clear-sky aerosol direct radiative effect in an alpine valley, by the synergy of ground-based measurements and radiative transfer simulations. *Bulletin of Atmospheric Science and Technology*, *2*(1–4), 1–24. https://doi.org/10.1007/s42865-021-00041-w

Goswami, B. N., Venugopal, V., Sengupta, D., Madhusoodanan, M., & Xavier, P. K. (2006). Increasing trend of extreme rain events over India in a warming environment. *Science*, *314*(5804), 1442–1445. https://doi.org/10.1126/science.1132027

Herbert, R., Stier, P., & Dagan, G. (2021). Isolating large-scale smoke impacts on cloud and precipitation processes over the amazon with convection permitting resolution. *Journal of Geophysical Research: Atmospheres*, *126*(13), e2021JD034615. https://doi.org/10.1029/2021jd034615

Holben, B. N., Tanré, D., Smirnov, A., Eck, T., Slutsker, I., Abuhassan, N., et al. (2001). An emerging ground-based aerosol climatology: Aerosol optical depth from aeronet. *Journal of Geophysical Research*, *106*(D11), 12067–12097. https://doi.org/10.1029/2001jd900014

Iacono, M. J., Delamere, J. S., Mlawer, E. J., Shephard, M. W., Clough, S. A., & Collins, W. D. (2008). Radiative forcing by long-lived greenhouse gases: Calculations with the AER radiative transfer models. *Journal of Geophysical Research*, *113*(D13), D13103. https://doi.org/10.1029/2008jd009944

Jakob, C., Singh, M., & Jungandreas, L. (2019). Radiative convective equilibrium and organized convection: An observational perspective. *Journal of Geophysical Research: Atmospheres*, *124*(10), 5418–5430. https://doi.org/10.1029/2018jd030092

Khairoutdinov, M. F. (2023). SAM model code [Software]. *MSCRC*. Retrieved from http://rossby.msrc.sunysb.edu/~marat/index.html

Khairoutdinov, M. F., & Randall, D. A. (2003). Cloud resolving modeling of the arm summer 1997 iop: Model formulation, results, uncertainties, and sensitivities. *Journal of the Atmospheric Sciences*, *60*(4), 607–625. https://doi.org/10.1175/1520-0469(2003)060<0607:crmota>2.0.co;2

Kim, H., Kang, S. M., Hwang, Y.-T., & Yang, Y.-M. (2015). Sensitivity of the climate response to the altitude of black carbon in the northern subtropics in an aquaplanet GCM. *Journal of Climate*, *28*(16), 6351–6359. https://doi.org/10.1175/jcli-d-15-0037.1

Kinne, S., O'Donnel, D., Stier, P., Kloster, S., Zhang, K., Schmidt, H., et al. (2013). Mac-v1: A new global aerosol climatology for climate studies. *Journal of Advances in Modeling Earth Systems*, *5*(4), 704–740. https://doi.org/10.1002/jame.20035

kumar Kopparapu, R., Wolf, E. T., Haqq-Misra, J., Yang, J., Kasting, J. F., Meadows, V., et al. (2016). The inner edge of the habitable zone for synchronously rotating planets around low-mass stars using general circulation models. *The Astrophysical Journal*, *819*(1), 84. https://doi.org/10.3847/0004-637x/819/1/84

Li, J., Barker, H., Yang, P., & Yi, B. (2015). On the aerosol and cloud phase function expansion moments for radiative transfer simulations. *Journal of Geophysical Research: Atmospheres*, *120*(23), 12–128. https://doi.org/10.1002/2015jd023632

Li, Z., Wang, Y., Guo, J., Zhao, C., Cribb, M. C., Dong, X., et al. (2019). East Asian study of tropospheric aerosols and their impact on regional clouds, precipitation, and climate (east-aircpc). *Journal of Geophysical Research: Atmospheres*, *124*(23), 13026–13054. https://doi.org/10.1029/2019jd030758

Liu, L., Shawki, D., Voulgarakis, A., Kasoar, M., Samset, B., Myhre, G., et al. (2018). A PDRMIP multimodel study on the impacts of regional aerosol forcings on global and regional precipitation. *Journal of Climate*, *31*(11), 4429–4447. https://doi.org/10.1175/jcli-d-17-0439.1

Lorian, S., & Dagan, G. (2023). On the sensitivity of aerosol-cloud interactions to changes in sea surface temperature in radiative-convective equilibrium. *EGUsphere*, *2023*, 1–20.

Lu, Q., Liu, C., Zhao, D., Zeng, C., Li, J., Lu, C., et al. (2020). Atmospheric heating rate due to black carbon aerosols: Uncertainties and impact factors. *Atmospheric Research*, *240*, 104891. https://doi.org/10.1016/j.atmosres.2020.104891

McCoy, I. L., Vogt, M. A., & Wood, R. (2022). Absorbing aerosol choices influences precipitation changes across future scenarios. *Geophysical Research Letters*, *49*(8), e2022GL097717. https://doi.org/10.1029/2022gl097717

Ming, Y., Ramaswamy, V., & Persad, G. (2010). Two opposing effects of absorbing aerosols on global-mean precipitation. *Geophysical Research Letters*, *37*(13), L13701. https://doi.org/10.1029/2010gl042895

Mlawer, E. J., Taubman, S. J., Brown, P. D., Iacono, M. J., & Clough, S. A. (1997). Radiative transfer for inhomogeneous atmospheres: RRTM, a validated correlated-k model for the longwave. *Journal of Geophysical Research*, *102*(D14), 16663–16682. https://doi.org/10.1029/97jd00237

Morrison, H., Curry, J., & Khvorostyanov, V. (2005). A new double-moment microphysics parameterization for application in cloud and climate models. Part I: Description. *Journal of the Atmospheric Sciences*, *62*(6), 1665–1677. https://doi.org/10.1175/jas3446.1

Muller, C. J., & Held, I. M. (2012). Detailed investigation of the self-aggregation of convection in cloud-resolving simulations. *Journal of the Atmospheric Sciences*, *69*(8), 2551–2565. https://doi.org/10.1175/jas-d-11-0257.1

Myhre, G., Kramer, R., Smith, C., Hodnebrog, Ø., Forster, P., Soden, B., et al. (2018). Quantifying the importance of rapid adjustments for global precipitation changes. *Geophysical Research Letters*, *45*(20), 11–399. https://doi.org/10.1029/2018gl079474

O'Gorman, P. A., Allan, R. P., Byrne, M. P., & Previdi, M. (2012). Energetic constraints on precipitation under climate change. *Surveys in Geophysics*, *33*(3–4), 585–608. https://doi.org/10.1007/s10712-011-9159-6

Pendergrass, A. G., Lehner, F., Sanderson, B. M., & Xu, Y. (2015). Does extreme precipitation intensity depend on the emissions scenario? *Geophysical Research Letters*, *42*(20), 8767–8774. https://doi.org/10.1002/2015gl065854

Persad, G. G. (2023). The dependence of aerosols' global and local precipitation impacts on the emitting region. *Atmospheric Chemistry and Physics*, *23*(6), 3435–3452. https://doi.org/10.5194/acp-23-3435-2023

Persad, G. G., Ming, Y., & Ramaswamy, V. (2012). Tropical tropospheric-only responses to absorbing aerosols. *Journal of Climate*, *25*(7), 2471–2480. https://doi.org/10.1175/jcli-d-11-00122.1

Popp, M., Schmidt, H., & Marotzke, J. (2016). Transition to a moist greenhouse with CO_2 and solar forcing. *Nature Communications*, *7*(1), 10627. https://doi.org/10.1038/ncomms10627

Ricchiazzi, P., Yang, S., Gautier, C., & Sowle, D. (1998). SBDART: A research and teaching software tool for plane-parallel radiative transfer in the Earth's atmosphere. *Bulletin of the American Meteorological Society*, *79*(10), 2101–2114. https://doi.org/10.1175/1520-0477(1998)079<2101:sarats>2.0.co;2

Samset, B. H. (2022). Aerosol absorption has an underappreciated role in historical precipitation change. *Communications Earth & Environment*, *3*(1), 242. https://doi.org/10.1038/s43247-022-00576-6

Sand, M., Samset, B. H., Tsigaridis, K., Bauer, S. E., & Myhre, G. (2020). Black carbon and precipitation: An energetics perspective. *Journal of Geophysical Research: Atmospheres*, *125*(13), e2019JD032239. https://doi.org/10.1029/2019jd032239

Seeley, J. T., & Wordsworth, R. D. (2021). Episodic deluges in simulated hothouse climates. *Nature*, *599*(7883), 74–79. https://doi.org/10.1038/s41586-021-03919-z

Shi, S., Cheng, T., Gu, X., Guo, H., Wu, Y., & Wang, Y. (2019). Biomass burning aerosol characteristics for different vegetation types in different aging periods. *Environment International*, *126*, 504–511. https://doi.org/10.1016/j.envint.2019.02.073

Sillmann, J., Stjern, C. W., Myhre, G., Samset, B. H., Hodnebrog, Ø., Andrews, T., et al. (2019). Extreme wet and dry conditions affected differently by greenhouse gases and aerosols. *npj climate and atmospheric science*, *2*(1), 24. https://doi.org/10.1038/s41612-019-0079-3

Slater, J., Coe, H., McFiggans, G., Tonttila, J., & Romakkaniemi, S. (2022). The effect of BC on aerosol–boundary layer feedback: Potential implications for urban pollution episodes. *Atmospheric Chemistry and Physics*, *22*(4), 2937–2953. https://doi.org/10.5194/acp-22-2937-2022

Song, X., Abbot, D. S., & Yang, J. (2023). Critical role of vertical radiative cooling contrast in triggering episodic deluges. In *small-domain hothouse climates*. arXiv preprint arXiv:2307.01219.

Spaulding-Astudillo, F. E., & Mitchell, J. L. (2023). The emergence of relaxation-oscillator convection on Earth and Titan. arXiv preprint arXiv:2306.03219.

Stevens, B., Fiedler, S., Kinne, S., Peters, K., Rast, S., Müsse, J., et al. (2017). MACv2-SP: A parameterization of anthropogenic aerosol optical properties and an associated Twomey effect for use in CMIP6. *Geoscientific Model Development*, *10*(1), 433–452. https://doi.org/10.5194/gmd-10-433-2017

Stjern, C. W., Hodnebrog, Ø., Myhre, G., & Pisso, I. (2023). The turbulent future brings a breath of fresh air. *Nature Communications*, *14*(1), 3735. https://doi.org/10.1038/s41467-023-39298-4

Stjern, C. W., Samset, B. H., Myhre, G., Forster, P. M., Hodnebrog, Ø., Andrews, T., et al. (2017). Rapid adjustments cause weak surface temperature response to increased black carbon concentrations. *Journal of Geophysical Research: Atmospheres*, *122*(21), 11–462. https://doi.org/10.1002/2017jd027326

Tabari, H. (2020). Climate change impact on flood and extreme precipitation increases with water availability. *Scientific Reports*, *10*(1), 13768. https://doi.org/10.1038/s41598-020-70816-2

Twomey, S. (1959). The nuclei of natural cloud formation Part II: The supersaturation in natural clouds and the variation of cloud droplet concentration. *Geofisica pura e applicata*, *43*(1), 243–249. https://doi.org/10.1007/bf01993560

Wang, T., Zhuang, B., Li, S., Liu, J., Xie, M., Yin, C., et al. (2015). The interactions between anthropogenic aerosols and the East Asian summer monsoon using RegCCMS. *Journal of Geophysical Research: Atmospheres*, *120*(11), 5602–5621. https://doi.org/10.1002/2014jd022877

Wang, Z., Huang, X., & Ding, A. (2018). Dome effect of black carbon and its key influencing factors: A one-dimensional modelling study. *Atmospheric Chemistry and Physics*, *18*(4), 2821–2834. https://doi.org/10.5194/acp-18-2821-2018

Wilcox, E. M., Thomas, R. M., Praveen, P. S., Pistone, K., Bender, F. A.-M., & Ramanathan, V. (2016). Black carbon solar absorption suppresses turbulence in the atmospheric boundary layer. *Proceedings of the National Academy of Sciences*, *113*(42), 11794–11799. https://doi.org/10.1073/pnas.1525746113

Williams, A. I., Watson-Parris, D., Stier, P., & Dagan, G. (2023). Dependence of fast changes in global and local precipitation on the geographical location of aerosol absorption. *Authorea Preprints*.

Wing, A. A., Reed, K. A., Satoh, M., Stevens, B., Bony, S., & Ohno, T. (2018). Radiative–convective equilibrium model intercomparison project. *Geoscientific Model Development*, *11*(2), 793–813. https://doi.org/10.5194/gmd-11-793-2018

Wolf, E., Haqq-Misra, J., & Toon, O. (2018). Evaluating climate sensitivity to CO_2 across earth's history. *Journal of Geophysical Research: Atmospheres*, *123*(21), 11–861. https://doi.org/10.1029/2018jd029262

Wolf, E., & Toon, O. (2015). The evolution of habitable climates under the brightening sun. *Journal of Geophysical Research: Atmospheres*, *120*(12), 5775–5794. https://doi.org/10.1002/2015jd023302

Zhang, S., Stier, P., & Watson-Parris, D. (2021). On the contribution of fast and slow responses to precipitation changes caused by aerosol perturbations. *Atmospheric Chemistry and Physics*, *21*(13), 10179–10197. https://doi.org/10.5194/acp-21-10179-2021